FEEDBACK DTC-SVM BASED A FRACTIONAL PI CONTROLLER: APPLIED TO ROTOR'S SPEED OF INDUCTION MOTOR

Zennir Youcef[(a)], Bouras Lakhdar[(b)]

[(a)] Automatic Laboratory of Skikda, Route El-Hadeaik, BP26. 21000 Skikda, Algeria
[(b)] Electrical Engineering Laboratory of Skikda, Route El-Hadeaik, BP26. 21000 Skikda, Algeria

[(a)]youcef.zennir@univ-skikda.dz, [(b)] bouras_nour@yahoo.fr

ABSTRACT
In this paper we present a new DTC approach for induction motor control , the approach is based on the use of both classical PI and fractional PI controllers , classical PI is used to control the magnetic flux and the torque whereas Fractional PI controller is used for rotor's speed control. In the first part we pointed out some structures of DTC control along with mathematical modeling for induction motor, in the second part a description of software simulation is given and finally we end up with discussion of obtained results and prospective for future works.

Keywords: workstation design, work measurement, ergonomics, decision support system

1. INTRODUCTION

The induction motors are widely used in industrial drives because they are rugged, reliable and economical (Casadei,1996), (Bin-jun 2012). The induction motors are increasingly being used with variable-frequency drives in variable-speed services. In the other hand Squirrel cage induction motors are used in both fixed-speed and VFD applications. The rotor circuit for induction motor consists of conducting bars regularly distributed between two metal crowns forming the ends. Since the induction motor have no field winding, then it is necessary to provide magnetic energy for the motor. The power supply for the motor can be provided using two ways: from the electrical network or a renewable energy sources. In the first case and in the upstream of the motor generally there is a rectifier and an inverter circuits to convert the continuous feed to alternative. The speed of the motor depends on the frequency, the number of pole's pairs, as well as the torque opposed by its load. If the motor is supplied from renewable energy source we only find an inverter, in the motor upstream (Jadhav 2011). In these two configurations the control of inverter frequency is needed ensure a good performance of the motor. The use of voltage inverter was the subject of many researches and it is necessary in this case to mention that the appearance of thyristor controller GTO and, thereafter, transistors IGBT help in the development of powerful, reliable MLI and with low costs voltage inverters (Jadhav 2011; Depenbrock 1988), which solve the problem associated to motor's feed, knowing that the control of the induction motor can be applied in steady state conditions. In the literature, there exist several works concerning the development new strategies that allow a control uncoupled from the motor with induction. Among these methods there are the field-oriented controls (FOC) which, ensure of the dynamic performances equivalent to those obtained by the motor with D.C. current (Bettou 2008). During last years, the development of new signal processing methods allow the realization of more advanced control structures, as example we mention the direct torque control (DTC), the synoptic ones of the order evolved certainly in the direction to improve some aspects like minimization of the influence of the motor parameters without requiring a mechanical sensor speed (Dingy 2006).

2. CLASSICAL DIRECT TORQUE CONTROL APPROACH

This control approach is based on the direct control of induction motor's torque. This approach was proposed by I. Takahashi and T. Noguchi (Chikh 2011) and Depenbrock (Mansour 2012). This control approaches the torque by the application of the inverter's with various voltage vectors, which determines its state. The control variables are the magnetic stator flux and the electromagnetic torque which are usually ordered by hysteresis controllers. The problem is how we can maintain the magnitude of stator flux and electromagnetic torque inside these bands of hysteresis controller. The output of these controllers determines the optimal tension vector to apply every moment at commutation. The use of this controller's type supposes the existence of a variable commutation frequency in the converter requiring a very weak step of calculation. The use of voltage inverter makes it possible to reach six distinct positions in the plan from phase, corresponding to the eight tension vector sequences on the outlet inverter side. The application of this approach gives a very fast dynamic response torque's motor. It seeks for obtaining the flux and the stator currents close to the sinusoidal forms. The commutation's frequency inverter depends on the hysteresis magnitude bands. The basic

structure of the direct torque control is presented on the following figure:

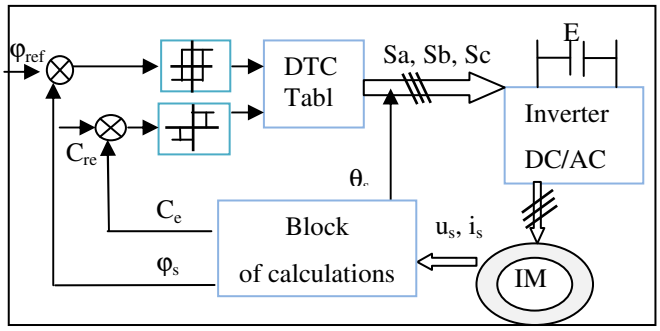

Figure 1: Architecture of classic DTC control.

The basic disadvantages of DTC classic approach using hysteresis controllers are the variable switching frequency, the current and torque ripple. The movement of stator flux vector during the changes of cyclic sectors is responsible for creating notable edge oscillations of electromagnetic torque. We can see also another great issue is the implementation of hysteresis controllers which requires a high sampling frequency. When a hysteresis controller is implemented its digital operation is quite different to the analogue one. In the analogue operation the value of the torque and the magnitude of the flux are limited in the exact desirable hysteresis band. That means, the inverter voltage can change state each time the torque or the flux magnitude are throwing the specified limits. The digital implementation uses specific sample time on which the magnitudes of torque and flux are checked to be in the desirable limits. That means, very often, torque and flux can be out of the desirable limits until the next sampling period. For this reason, an undesirable torque and flux ripple is observed. (Depenbrock 1988). During the last years, a lot of developments and modifications in classic Direct Torque Control approach of control applied of induction motor control (Chikh 2011), have been made. The objective of these modifications was to improve the motor's start up. Also our modifications proposed aimed to reduce the torque and current ripple and to avoid the variable switching frequency. Then we focused our study to develop new control's architecture for switching frequency control and to return it as possible constant in DTC closed loop structure. This new structure of control based on the space vector modulation (SVM) for voltage inverter control and different standard controller (classic and fractional PI) to improve the performances of the motor and to solve the problems of the classic DTC

3. FEEDBACK DTC CONTROL WITH PI CONTROLLER

This type of control use space vector modulation (SVM) to inverter control and PI controller for electromagnetic Torque and the magnetic flux control (Ortega 2005; Casadei 2000). With this approach we have constant switch frequency; it improves the dynamic and the static response, and decreases also the undulations of torque and the current. These results are more interesting then obtain with classic DTC, but it's more complicated than the classic DTC. The algorithm of this new control with rotor's speed control is represented by the following figure.

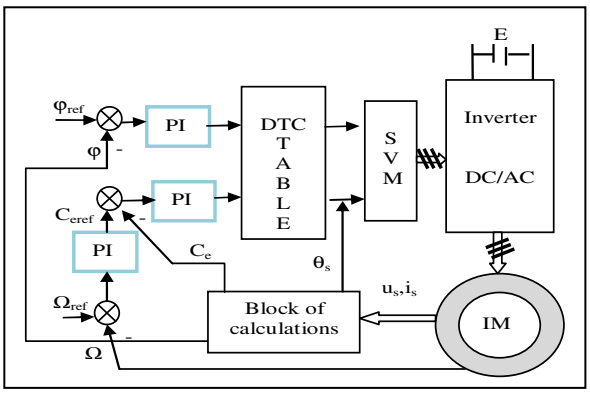

Figure 2: Feedback DTC control with PI controller.

We describing in the following section the synthesis of classic PI controller used to control magnetic flux, the electromagnetic torque and rotor's speed.

3.1. DTC-SVM control with classic PI controller

The mathematical model for induction motor is described by the following equations (Bouras 2005):

- Electric equations (stator's and rotor's voltages):

$$V_{sd} = R_s \cdot I_{sd} + \frac{d}{dt}\varphi_{sd} - \omega_s \cdot \varphi_{sq} \quad (1)$$

$$V_{sq} = R_s \cdot I_{sq} + \frac{d}{dt}\varphi_{sq} + \omega_s \cdot \varphi_{sd} \quad (2)$$

$$V_{rd} = R_r \cdot I_{rd} + \frac{d}{dt}\varphi_{rd} - (\omega_s - \omega_r) \cdot \varphi_{rq} = 0 \quad (3)$$

$$V_{rq} = R_r \cdot I_{rq} + \frac{d}{dt}\varphi_{rq} + (\omega_s - \omega_r) \cdot \varphi_{rd} = 0 \quad (4)$$

- Magnetic flux equations:

$$\varphi_{sd} = L_s \cdot I_{sd} + L_M \cdot I_{rd} \qquad \varphi_{sq} = L_s \cdot I_{sq} + L_M \cdot I_{rq} \quad (5)$$
$$\varphi_{rd} = L_r \cdot I_{rd} + L_M \cdot I_{sd} \qquad \varphi_{rq} = L_r \cdot I_{rq} + L_M \cdot I_{sq}$$

3.2. Control of stator flux

The induction motor have nonlinear mathematical model represented by the coupling between the torque and magnetic flux. Then for linearization of this model, we decouple the torque and magnetic flux, by the orientation of magnetic flux according to direct "D" component. Which gives $\varphi_{sd} = \varphi_s$ and $\varphi_{sq} = 0$. And then applying this in the above equations we get the following model:

$$V_{sd} = R_s \cdot I_{sd} + \frac{d}{dt}\varphi_s \; ; \quad V_{sq} = R_s \cdot I_{sq} + \omega_s \cdot \varphi_s \quad (6)$$

$$C_e = \frac{3}{2} \cdot p \cdot \varphi_s \cdot I_{sq} \quad (7)$$

$$I_{rd} = \frac{1}{L_M} \cdot (\varphi_s - L_s \cdot I_{sd}); \qquad I_{rq} = -\frac{L_s}{L_M} \cdot I_{sq} \quad (8)$$

$$\varphi_{rd} = \frac{L_r}{L_M} \cdot (\varphi_s - \sigma \cdot L_s \cdot I_{sd}) \varphi_{rq} = -\sigma \cdot \frac{L_s \cdot L_r}{L_M} \cdot I_{sq} \quad (9)$$

With: $\sigma = 1 - \frac{L_M^2}{L_s \cdot L_r}$

With (7) and (8) in (9) we obtain

$$\varphi_s = \frac{L_s\cdot[(1+\sigma\cdot T_r\cdot S)\cdot I_{sd}+\sigma\cdot T_r\cdot I_{sq}\cdot\omega_{sl}]}{1+T_r\cdot S} \quad (10)$$

$$I_{sq} = \frac{T_r\cdot\omega_{sl}[\varphi_s-\sigma\cdot L_s\cdot I_{sd}]}{L_s\cdot(1+\sigma\cdot T_r\cdot S)} \quad (11)$$

With: $T_r = \frac{L_r}{R_r}$

From (10) and (11) we obtain:

$$V_{sd} = \frac{\varphi_s}{G_{\varphi_s}} + E_d \quad (12)$$

$V_{sq} = R_s\cdot I_{sq} + \omega_s\cdot\varphi_s$. The term $R_s\cdot I_{sq}$ it's very small then: $V_{sq} \cong \omega_s\cdot\varphi_s$

$$G_{\varphi_s} = \frac{T_s\cdot(1+\sigma\cdot T_r\cdot S)}{1+(T_r+T_s)\cdot S+\sigma\cdot T_r\cdot T_s\cdot S^2} \quad E_d = -\frac{\sigma\cdot R_s\cdot T_r\cdot I_{sq}\cdot\omega_{sl}}{1+(T_r+T_s)\cdot S} \quad (13)$$

Hence we can control stator's magnetic flux by the component d of the stator's tension. And we have a system of second degree with disturbance Ed represented by the following block diagram:

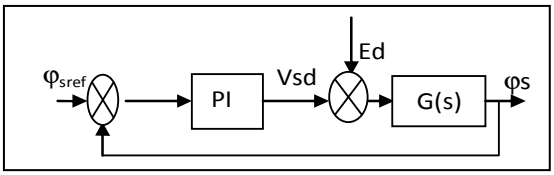

Figure 3: Block diagram of the flux loop

3.3. Torque control

To control the torque we have:

$$\varphi_s = \frac{L_s\cdot[(1+\sigma\cdot T_r\cdot S)\cdot I_{sd}+\sigma\cdot T_r\cdot I_{sq}\cdot\omega_{sl}]}{1+T_r\cdot S} \quad (15)$$

$$I_{sq} = \frac{T_r\cdot\omega_{sl}[\varphi_s-\sigma\cdot L_s\cdot I_{sd}]}{L_s\cdot(1+\sigma\cdot T_r\cdot S)} \quad (16)$$

From where:

$$I_{sd} = \frac{(1+T_r\cdot S)\cdot\varphi_s-\omega_{sl}\cdot\sigma\cdot L_s\cdot T_r\cdot I_{sq}}{L_s\cdot(1+\sigma\cdot T_r\cdot S)} \quad (17)$$

$$I_{sq} = \frac{T_r\cdot\omega_{sl}}{L_s\cdot(1+\sigma\cdot T_r\cdot S)}\cdot\left[\varphi_s - \frac{\sigma\cdot L_s\cdot[(1+T_r\cdot S)\cdot\varphi_s-\omega_{sl}\cdot\sigma\cdot L_s\cdot T_r\cdot I_{sq}]}{L_s\cdot(1+\sigma\cdot T_r\cdot S)}\right] \quad (18)$$

$$I_{sq} = \frac{\frac{(1-\sigma)\cdot T_r}{(L_s)}\cdot{\varphi_s}^2\cdot\omega_{sl}}{(1+\sigma\cdot T_r\cdot S)^2+(\omega_{sl}\cdot\sigma\cdot T_r)^2} \quad (19)$$

While replacing in the formula of the torque we obtains:

$$C_e = \frac{3}{2}\cdot p\cdot\frac{\frac{(1-\sigma)\cdot T_r}{(L_s)}\cdot{\varphi_s}^2\cdot\omega_{sl}}{(1+\sigma\cdot T_r\cdot S)^2+(\omega_{sl}\cdot\sigma\cdot T_r)^2} \quad (20)$$

With: σ it's very small then

$$C_e = \frac{3}{2}\cdot p\cdot\frac{\frac{(1-\sigma)\cdot T_r}{(L_s)}{\varphi_s}^2}{1+2\cdot\sigma\cdot T_r\cdot S}\cdot(\omega_s-\omega_r) \quad (21)$$

$$C_e = G_{ce}(s)\cdot(\omega_s-\omega_r) \quad (22)$$

With: $$G_{ce}(s) = \frac{3}{2}\cdot p\cdot\frac{\frac{(1-\sigma)\cdot T_r}{(L_s)}}{1+2\cdot\sigma\cdot T_r\cdot S}\cdot{\varphi_s}^2 \quad (23)$$

From the above equations we conclude that we can control the electromagnetic torque by the stator's pulsation as it is indicated in the following block diagram:

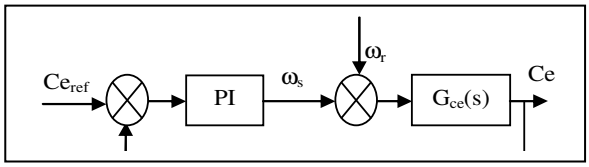

Figure 4: Block diagram of the torque loop

From the above block diagrams the control structure of DTC-SVM control with a classical PI controller is presented, in the next section we present the synthesis of a fractional PI controller for rotor's speed control.

3.4. DTC-SVM control with fractional PI controller for rotor's speed

The fractional PI controller has better flexibility in the operating concept because it has anther parameter that represents the fractional control of integral action in the PI controller. This parameter can be used to satisfy additional performances in the systems design controlled. For the adjustment fractional parameters controller PI^{α} (Kc, Ti, α) we us the following algorithm (Bettou 2008)(Bouras 2013):

Step1: calculate the parameters θi for $0 \ll i \ll 2$

$$\theta_0 = \frac{1}{2}\,;\theta_1 = \frac{-m}{4\cdot\omega_u}\,;\theta_2 = \frac{m}{4\cdot\omega_u^2} \quad (24)$$

With: ω_u : frequency of the profit unit of the reference model; m: the derivation fractional order of the reference model; θ_i : derived from the transfer function of the reference model Gd(p)

Step 2: calculate the parameters y_i for $0 \ll i \ll 2$

$$y_0 = \sum_{k=0}^{N} G_P(kT)\cdot e^{-K\cdot T\cdot\omega_u} \quad (25)$$

$$y_1 = -\sum_{k=0}^{N}(kT)\cdot G_P(kT)\cdot e^{-K\cdot T\cdot\omega_u} \quad (26)$$

$$y_2 = \sum_{k=0}^{N}(kT)^2\cdot G_P(kT)\cdot e^{-K\cdot T\cdot\omega_u} \quad (27)$$

With: y_i : derived from the transfer function Gp(p) compared to the variable p at the point ω_u; N : many samples.

Step 3: calculate the parameters $_{xi}$ for $0 \ll i \ll 2$

$$x_0 = \frac{\theta_0}{y_0\cdot(1-\theta_0)}\; x_1 = \frac{\theta_1}{y_0\cdot(1-\theta_0)^2} - \frac{x_0\cdot y_1}{y_0} \quad (28)$$

$$x_2 = \frac{\theta_2}{y_0\cdot(1-\theta_0)^2} + \frac{2\cdot\theta_1^2}{y_0\cdot(1-\theta_0)^3} - \frac{2\cdot x_1\cdot y_1+x_0\cdot y_2}{y_0} \quad (29)$$

with : xi : derived from the transfer function of the controller C(p)

Step 4: calculate the parameters Kc, Ti, α

$$\alpha = -\frac{\omega_u\cdot x_2}{x_1} - 1\;;$$

$$T_i = -\frac{{\omega_u}^{(1+\alpha)}\cdot x_1}{\alpha};\; K_c = x_0 - T_i\cdot{\omega_u}^{-\alpha} \quad (30)$$

Concerning the approximation of fractional action we used the approximation method developed by Charef (Bettou 2008). The transfer function in closed loop for rotor's speed is regarded as stable. The problem system's design is thus to regulate the three parameters of fractional controller to guarantee that the transfer

function in closed loop behaves the frame of reference which itself answers the specifications of the fractional control system (transfer function in closed loop). The frame of reference fractional model used is:

$$G_d(p) = \frac{1}{1+\left(\frac{p}{\omega_u}\right)^m} \text{ avec } 1 < m < 2 \qquad (31)$$

4. SIMULATION

Our aim is studying the effectiveness of fractional PI controller and comparing the results with the use of traditional PI controller, We carried out the following simulations: DTC-SVM control with a classic PI controller for the torque, stator's magnetic flux and rotor's speed (in close loop), and DTC-SVM control with a fractional PI controller for the rotor's speed. All simulations developed in the Matlab-Simulink environment and the parameters of the controllers, induction motor and reference model are illustrated in the following table:

Table 1: Simulation's Parameters

	Parameters
PI	of magnetic flux : Kp=20 ; Ki= 200; of torque: Kp=5 ; Ki=20 ;
PI^{α}	α= 0.5; Kp= 0.46; Ki= 3.2;
IM	Nominal power 1.5k W , J = 0.013 $Kg.m^2$
	Rs=4.75 Ω , Rr=6.3 Ω ; Lm=0.612 H
	Ls=0.6550 H , Lr=0.6520 H ; P = 4
	Coefficient of friction F = 0.002 Nms
Reference model :	ω=10 rd/s; ξ=0.707

The transfers function of fractional PI controller:

$$G_{PI^{\alpha}}(p) = k_p * \left(1 + k_i * G1(p)\right) = \frac{num(p)}{den(p)} \qquad (32)$$

Degrees of the num (p) =26 and den (p) =28 with zeros and poles distinguish. The results obtained are illustrated in the following figures:

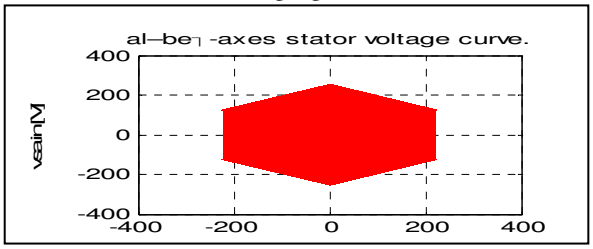

Figure 5: Stator voltage curve with classical PI.

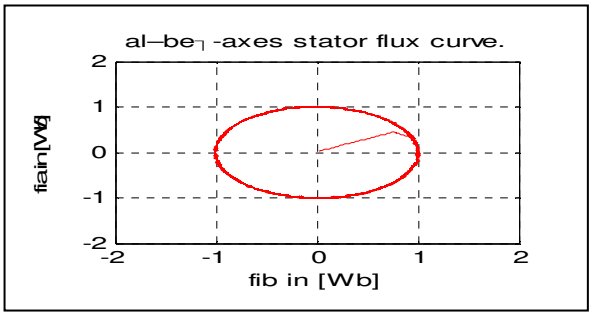

Figure 6: Stator magnetic flux curve with classical PI.

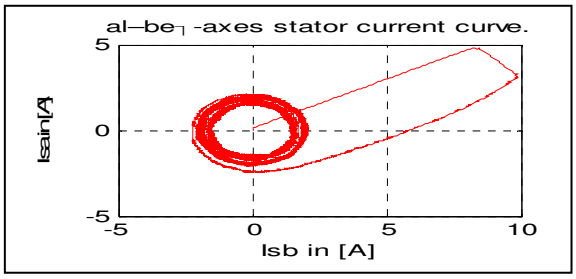

Figure 7: Stator current curve with classical PI.

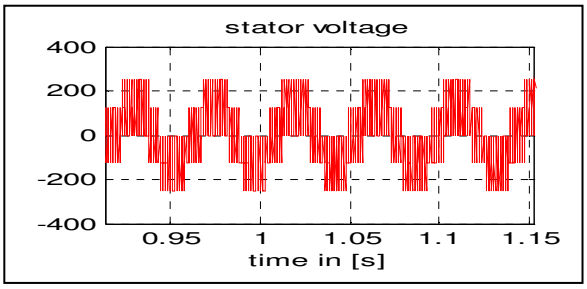

Figure 8: Stator voltage with classical PI.

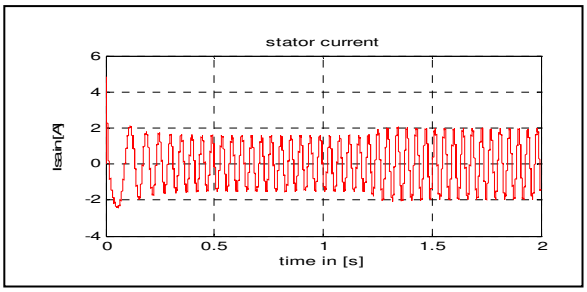

Figure 9: Stator current with classical PI.

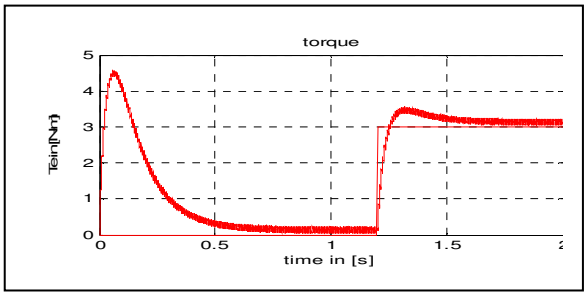

Figure 10: Torque with classical PI.

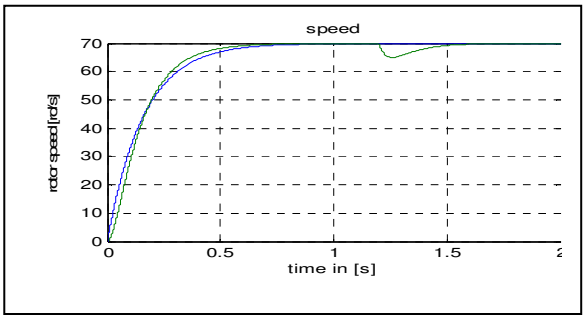

Figure 11: Rotoric Speed with classical PI.

5.

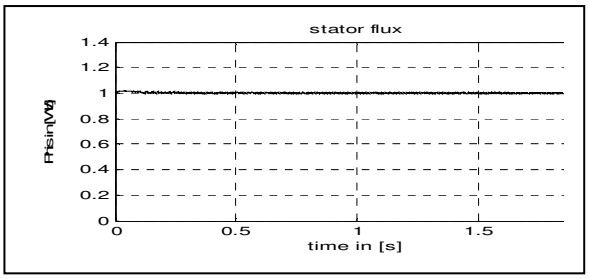

Figure 12: Stator magnetic flux with classical PI.

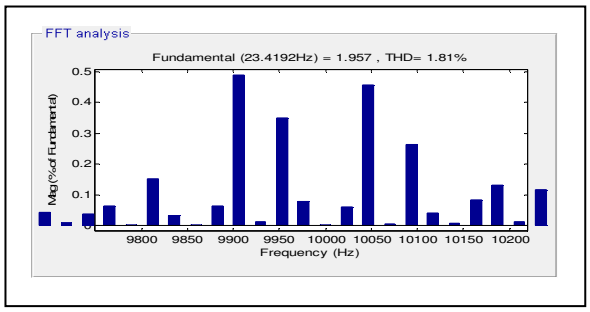

Figure 13: FFT of stator current with classical PI.

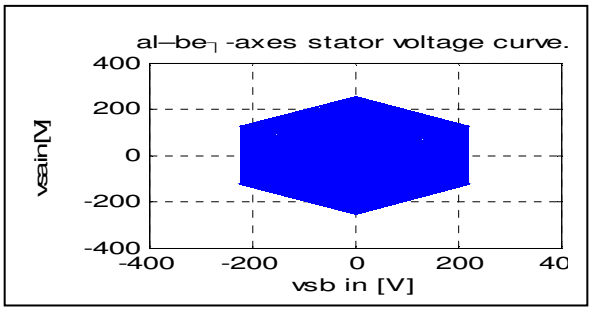

Figure 14: Stator voltage curve with fractional PI.

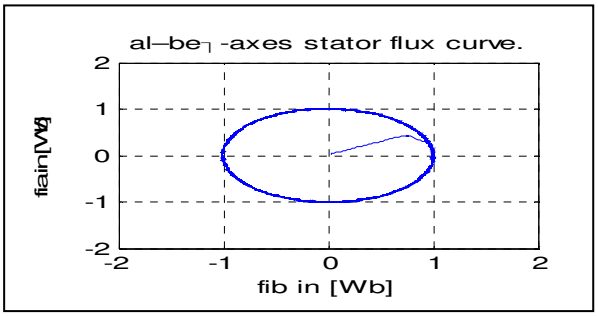

Figure 15: Stator magnetic flux curve with fractional PI.

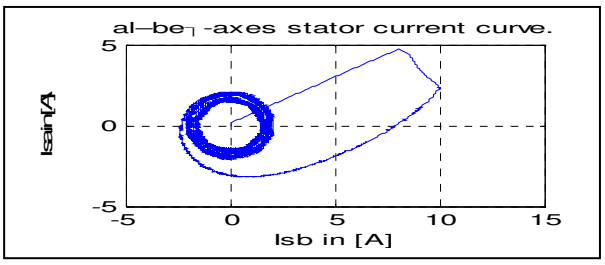

Figure 16: Stator current curve with fractional PI.

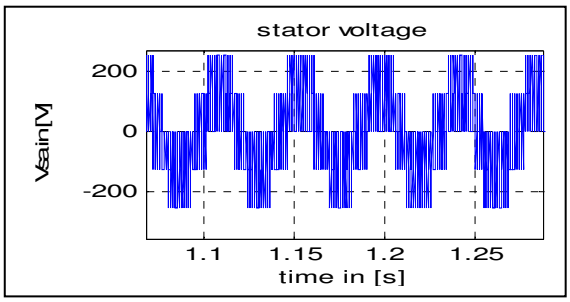

Figure 17: Stator voltage with fractional PI.

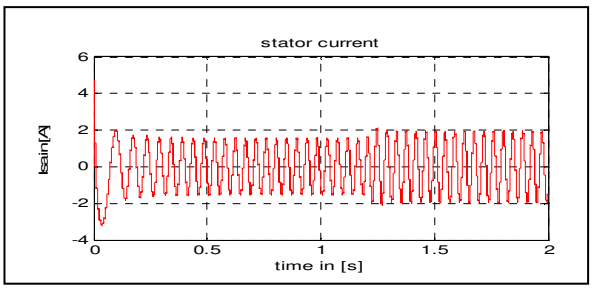

Figure 18: Stator current with fractional PI.

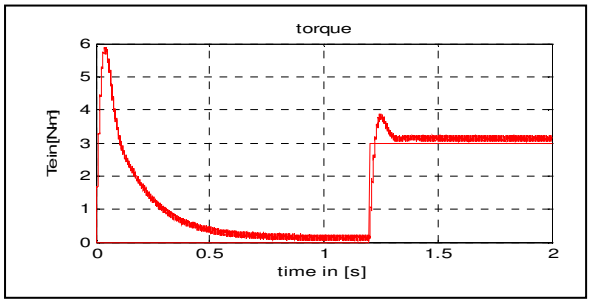

Figure 19: Torque with fractional PI.

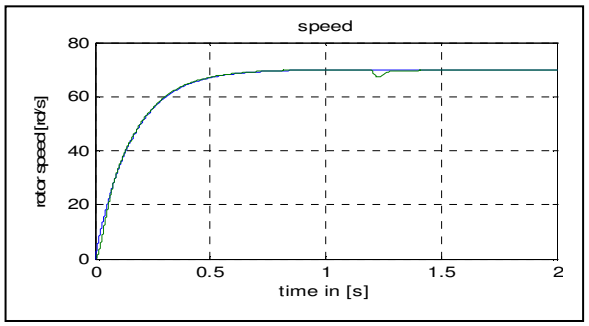

Figure 20: Rotoric Speed with fractional PI.

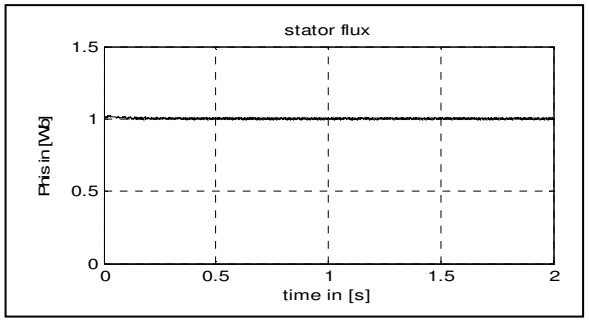

Figure 21: Stator flux with fractional PI.

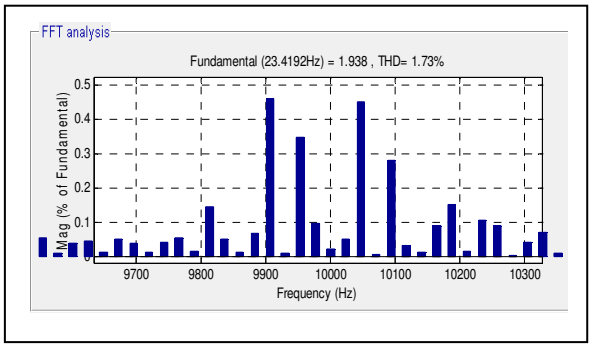

Figure 22: FFT of stator current with fractional PI.

The simulations results obtained starting from the DTC-SVM with classic PI controller applied to electromagnetic torque, flux magnetic and rotor's speed are illustrated in Figure 5 to 13. Figure 14 to 22 show the results obtained with fractional PI controller applied for rotor's speed in DTC-SVM control. We note that the results obtained with classic PI are more interesting than classic DTC (8)(9) and switch frequency is constant f=10 kHz. We also notice that all results obtained with PI fractional applied in rotor's speed is more interesting then obtained with classic PI and the correction is more quickly with fractional PI controller (figure 20). We can also see that fractional PI controller gives good performances compared to classic PI and when the harmonic content (THD) is weaker (compared between figure 13 and figure 22), the form of the stator's current is closer to the form of a sinusoidal signal (figure 18).

CONCLUSION

We presented in this paper a new approach of DTC control. We use in this approach the space vector modulation applied to the voltage's inverter, PI classic controller of torque and stator's flux and classic or fractional PI controller applied in the rotor's speed. According to the results obtained and the remarks observed before, we can conclude that the DTC-SVM with a fractional PI controller it's more efficient then DTC-SVM used classic PI controller for rotor's speed on the level of precision, response time and the robustness. Nevertheless there are some remaining points that should be considered in the future work for example the choice between the null vectors (V0 and V7) and to validate this control with PI fractional controller for torque, flux magnetic and rotor's speed.

REFERENCES

Casadei, D. Serra, G. and Tani. A. 1996. Constant frequency operation of a DTC induction motor drive for electric vehicule. Sept, 10-12, pp.224-229 In proc, ICEM'96, vol.III, Vigo, Spain,.

Bin-jun, C. Xiao hong, N., 2012. A Novel MC-DTC Method for Induction Motor Based on Fuzzy-neural Network Space Vector Modulation. Journal of software, Vol. 7, N° 5, May 2012, pp 966-973.

Jadhav, S. V. Mohan Krishna Reddy, M., and Chaudhari, B. N. 2011. An Improved SVM-DTC based Induction Motor Drive Scheme using d-SPACE. pp 388-393. IEEE PEDS, Singapore,

Depenbrock, D., 1988. Direct self control of inverter-fed induction motor. IEEE Trans. Power Electron. Vol. (3), pp.420-429.

Takahashi, I. and Noguchi, T., 1986. A new quick-response and high efficiency control strategy of an induction motor. IEEE Trans. Ind. Applicant., Vol. (22). pp.820-827.

Bettou, K. Charef, K.A, 2008. A New design method for fractional PIλDμ controller, IJSTA, vol.2, N° 1, pp 414-429.

Dingy, X. Chunna, Z., and Yang, Q.C., 2006. A Modified Approximation Method of Fractional Order System. pp.1043- 1048. IEEE International Conference on Mechatronics and Automation, June 25 - 28, 2006, Luoyang, China, ,

Mansour, M. Rachdi, S., Mansouri, M. N., Mimouni, M. F. 2012. Direct Torque Control Strategy of an Induction-Motor-Based Flywheel Energy Storage System Associated to a Variable-Speed Wind Generator. Journal of Energy and Power Engineering, Vol. (4), pp. 255-263.

Chikh, K. Saad, A. Khafallah, M. and Yousfi, D. 2011. A Novel Drive Implementation for PMSM By using Direct Torque Control with Space Vector Modulation. Canadian Journal on Electrical and Electronics Engineering, Vol.(2), pp. 400-408.

L. Bouras, Y. Zennir and F. Bourourou. 2013. Direct torque control with SVM based a fractional controller : Applied to the induction motor. Proceeding of the 3rd internaional conference on system and control pp.702-707. 978-1-4799-0275-0/13/$3100 © IEEE, 29-31 October. Algeria.

Ortega, M., & al., 2005. Direct Torque Control of Induction Motors using Fuzzy Logic with current limitation, IEEE Industrial Electronics Society, IECON. 32nd Annual Conference.

Casadei, D. & al. 2000. Implementation of a Direct Torque Control Algorithm for Induction Motors Based on Discrete Space Vector Modulation, IEEE Trans. Ind. Applicat. vol. 15, No.4 pp. 769–777.

L. Bouras, M. Kadjoudj, N. Golea. 2005. Contrôle Direct du Torque Basé sur la Modulation Vectorielle avec Régulateurs à Hystérésis Appliqué à la Motor à Induction. pp 319-324. First International Conference on Electrical Systems, PCSE'05, May 9-11, O. E. Bouaghi Univ. Algeria.